



The polyethylene glycol xanthate-mediated synthesis of block copolymers via novel MADIX agents containing azo initiator: Effect of PEG chain length on molecular properties

Umit Yildiko¹ · Ahmet Cagri Ata² · İsmail Cakmak² · Aslihan Aycan Tanriverdi²

Received: 13 December 2020 / Revised: 25 May 2021 / Accepted: 27 June 2021 /

Published online: 1 July 2021

© The Author(s), under exclusive licence to Springer-Verlag GmbH Germany, part of Springer Nature 2021

Abstract

Novel macro-xanthate agents containing azo initiator and polyethylene glycol (PEG) were synthesized to prepare block copolymers via macromolecular design by an interchange of xanthate (MADIX) polymerization. In this system, the multifunctional agents were used as both macromolecular chain transfer agents and free radical sources. Polystyrene–polyethylene glycol–polystyrene (PS-PEG-PS) copolymers were prepared easily with molecular weight (M_n) from 23,000 to 43,000 g/mol by MADIX copolymerization of styrene using PEG-N=N-PEG (M_n , PEG = 600, 1000, 1500, and 3000 g/mol) as the macro-MADIX agents. In this process, the molar mass (M_n) increased over time for a controlled MADIX polymerization process, but the polydispersity varied slightly. The controlled polymerizations showed typical living properties, and polymers having low polydispersity (below $\mathcal{D} < 1.4$) were obtained with well-defined macromolecular structures. As a result, the macro-MADIX agents and the azo-initiator macromolecules were performed successful formation of the block copolymers. The obtained block copolymers were characterized by gel permeation chromatography, differential scanning calorimetry, Fourier transform infrared spectroscopy, and hydrogen nuclear magnetic resonance ($^1\text{H NMR}$) spectroscopy.

Keywords RAFT · PEG · Macro-MADIX agents · Polydispersity · Block copolymers

✉ Umit Yildiko
yildiko1@gmail.com

¹ Architecture and Engineering Faculty, Department of Bioengineering, Kafkas University, Central Campus/Kars 36100, Turkey

² Faculty of Arts and Sciences, Department of Chemistry, Kafkas University, Kars 36100, Turkey

Introduction

Synthesis of the block copolymer in polymer chemistry is important due to the exploration of the new features of materials [1, 2]. Producing of well-defined block copolymers could be performed to make complex and usefully macromolecular structures by many polymerization techniques according to their advantages [3]. Reversible addition-fragmentation chain transfer (RAFT) polymerization became one of the most versatile synthesis techniques for living radical polymerizations [4–7]. RAFT polymerization is the most successful method among degenerative chain transfer polymerizations, such as nitroxide mediated polymerization (NMP) [8, 9] and atom transfer radical polymerization (ATRP) [10–12]. These all polymerization processes enable the researchers to control simultaneously the molecular weight and molecular weight distribution [13]. The main difference of ATRP or NMP from the RAFT is that RAFT is based on chain transfer agents (CTAs) [14]. Furthermore, the controlled/live free radical polymerization method provides excellent functional group tolerance and the advantage of controlling all radical polymerizable monomers [15–17]. After the reporting of the RAFT process, it has been described preparation of many different structures of RAFT agents, which are monofunctional, difunctional different dithioester structures, the xanthenes, etc. [11, 18–20]. Moreover, functional polymer structure required an effective RAFT agent, which has good homolytic leaving groups [21, 22]. This effective RAFT/MADIX agent design is very useful in the preparation of functional block copolymer [23–26], star [27], branched [28], surface modification, thermal and pH-sensitive, and similar architectures [19, 29]. Besides, the agents are required to well control polymer molecular weights and to obtain polymer material with low polydispersity, i.e., narrow molecular weight distribution [30, 31]. Recently, our group synthesized macro-reversible addition-fragmentation termination (RAFT) agents based on poly(ethylene glycol)(PEG) [32]. RAFT polymerization of the styrene was carried out in the presence of these macro-RAFT agents and 2,2'-azobisisobutyronitrile (AIBN) to yield PS-*b*-PEG-*b*-PS block copolymers [33]. In recent years, PEG and its solutions are widely used as a beneficial reaction medium in many organic conversions due to their excellent profile, such as inexpensive, non-toxic, biodegradable, recyclable, and water soluble, which facilitates easy removal from the reaction product. In addition, replacing hazardous solvents with those that do not harm the environment is one of the main focus areas of green chemistry. Therefore, the use of green solvents like poly (ethylene glycols) (PEGs) is in great demand. In view of this, it has been found that polyethylene glycol (PEG) is an interesting solvent system. These attractive properties of PEG started using PEGs as the reaction medium at room temperature. According to the literature, one of the goals has been to examine the effect of PEG molecular weight (MW 600–3000 g/mol) on the reaction. The higher the MW of PEGs, the healthier the reaction will take place [34–36].

The use of azo initiators is common in radical polymerization [37–39]. Macro-azo initiators (MAI) are useful compounds used in the synthesis studies of the block copolymer. Cvetkovska et al. synthesized azo compounds containing

polyethylene glycol [40, 41]. Nakamura and his coworkers reported the preparation of polydimethylsiloxane-block-poly(methyl methacrylate) (PMMA) using polydimethylsiloxane-containing macro-azo initiator [42]. For vinyl monomers, it is possible to synthesize block copolymers using both the initiator and the polymer unit thereon [43]. The macro-azo initiators were sequenced with the polymer segment and the azo group. Therefore, new design polymers are produced with the effect of block groups [44]. Due to the solubility of macro-azo initiators, they are involved in many types of polymerization [45]. In our system, in addition to the above, as another advantage, we distinguish it from its toxicity by the elimination of the $-CN$ nitrile group on the 2,2'-azobisisobutyronitrile (AIBN), which we use to synthesize the azo initiator we produce. However, there are no reports in the literature about the synthesis of the chain transfer agent-containing azo initiator for RAFT/ MADIX polymerization.

In this study, we first synthesized the new functionalized xanthate agent called MCTA containing azo-initiator group and PEG blocks and then used it as an agent in styrene RAFT/MADIX polymerization to obtain well-defined statistical (PS-PEG-PS) block copolymers. Furthermore, we reported the synthesis of the RAFT/ MADIX agent containing a macro-azo-initiator group for the first time.

Materials and methods

Materials

Styrene was purchased from Merck and purified by a conventional procedure. The initiator, 2,2-azobis(isobutyronitrile) (AIBN) was recrystallized from toluene and stored in a refrigerator. PEGs having 600, 1000, 1500, and 3000 g/mol molecular weights were bought from Merck and used without further purification. Carbon disulfide (Merck, 99%), potassium hydroxide (Aldrich, 85%), benzoyl chloride (Aldrich, 99%), benzene (Aldrich, 99%), and styrene (Aldrich, 96%) were distilled under vacuum before use. (Aldrich, 96%), diethyl ether (Riedel–de Haen, 99,5), and petroleum ether (Riedel–de Haen, 99,5) were used as commercially supplied.

Characterization

Gel permeation chromatography (GPC) was used to determine the molecular weight (M_n) as well as polydispersity (D). GPC chromatograms were obtained using Waters 510 instrument by using THF as the solvent at a flow rate of 1 mL/min with a Waters 1515 isocratic HPLC pump equipped, a Waters 2414 refractive index detector, and 3 Waters Styragel HR columns. FT-IR spectra were recorded by a Bruker Alpha-P spectrometer for the polymer films cast from $CHCl_3$ solutions. NMR spectra of the products were taken by a Bruker Avance III NMR spectrometer in $CDCl_3$ solvent. Differential scanning calorimetry (DSC) measurements were obtained by Shimadzu 60 differential calorimeter in the changing temperature from 20 to 200 °C at a heating rate of 20 °C in a nitrogen atmosphere.

Synthesis of (MCTA1) with PEG 600

PEG 600 (24.05 g, 0.04 mol) and 15 mL benzene were added to a 500-mL flask equipped with a magnetic stirring bar, and the obtained mixture was dissolved. Followed by the addition of (2.24 g, 0.04 mol) KOH reaction to the flask, the mixture was stirred for 3 h. After adding $d=1.26 \text{ g/cm}^3$, 1.25 mL CS_2 reaction to the solution, it was stirred again for 16 h. After 16 h of stirring, a dark yellow–red solution was formed.

2.5 mL (0.02 mol) benzoyl chloride was added to the yellow product. The reaction solution was stirred with a magnetic bar for 9 h. After stirring, the viscous product was obtained and the light brown solution was filtrated by a filtration filter. The product was evaporated in an evaporator at 40 °C for 24 h. After evaporation of the solvent, the product was deposited in diethyl ether–petroleum ether (50–50%, 0 °C) and then was kept in the refrigerator for 1 day. The product was decanted and dried in the oven at 25 °C for 7–8 h.

PEG 600 synthesis of pinner (MCTA1)

Obtained 18.302 g (2) macro-RAFT agent and AIBN 0.9 g were mixed and the mixture was dissolved with benzene two-necked flask. HCl gas was passed through the system, and the reaction was initiated. For HCl gas, 80 g NaCl salt was added in two neck flask and dropwise H_2SO_4 was added. After the reaction, 1 g H_2O and NaHCO_3 were added to the reaction mixture for neutralization. The product was filtrated and evaporated in a vacuum evaporator at 40 °C for 24 h. After evaporation, solvent was deposited in diethyl ether–petroleum ether (50–50%, 0 °C) and kept in the refrigerator for 1 day. FT-IR (ν , cm^{-1}): 3069 (–C–H, Ar), 1674 (–C=O) 1086 (–C=S). ^1H NMR (CDCl_3 , δ , ppm): 7.9–7.6 (4H, ArH), 4.3 (2H, –OCH₂), 3.7–3.4 (4H, –CH₂CH₂–), ^{13}C NMR (CDCl_3 , δ , ppm): 167 (C=S), 163 (C=O), 143 (C–CH₃), 133–127 (Ar–C), 72 (O–CH₂), 60 (2C, –CH₂CH₂–), 28–26 (–CH₃) (Figure S1–S2).

Synthesis of PEG 1000 MAI—RAFT (MCTA2), PEG 1500 MAI—RAFT Agent (MCTA3), and PEG 3000 MAI—RAFT Agent (MCTA4)

40.3884 g (0.04 mol) PEG 1000, 17 mL benzene, 2.24 g (0.04 mol) KOH, $d=1.26 \text{ g/cm}^3$, 1.25 mL CS_2 , $d=1.21 \text{ g/cm}^3$ 2.5 mL (0.02 mol) benzoyl chloride. Yield (2) 23.604 g benzoyl chloride 1.6415 g AIBN. 60.5575 g (0.04 mol) PEG 1500, 15 mL benzene, 2.24 g (0.04 mol) KOH, $d=1.26 \text{ g/cm}^3$, 1.25 mL CS_2 , $d=1.21 \text{ g/cm}^3$ 2.5 mL (0.02 mol) benzoyl chloride. Yield (2) 45.85 g benzoyl chloride 1.6415 g AIBN. 60.3226 g (0.02 mol) PEG 1500, 15 mL benzene, 2.24 g (0.01 mol) KOH, $d=1.26 \text{ g/cm}^3$, 0.6 mL CS_2 , $d=1.21 \text{ g/cm}^3$ 1.15 mL (0.02 mol) benzoyl chloride. Yield (2) 49.5 g benzoyl chloride 1.2812 g AIBN. FT-IR (ν , cm^{-1}): MCTA2 için 3069 (–C–H, Ar), 1674 (–C=O) 1086 (–C=S), MCTA3 için 3069 (–C–H, Ar), 1674 (–C=O) 1086 (–C=S) ve MCTA4 için 3069 (–C–H, Ar), 1674 (–C=O) 1086 (–C=S). ^1H NMR (CDCl_3 , δ , ppm): MCTA2 için 7.9–7.5 (4H, ArH), 4.2

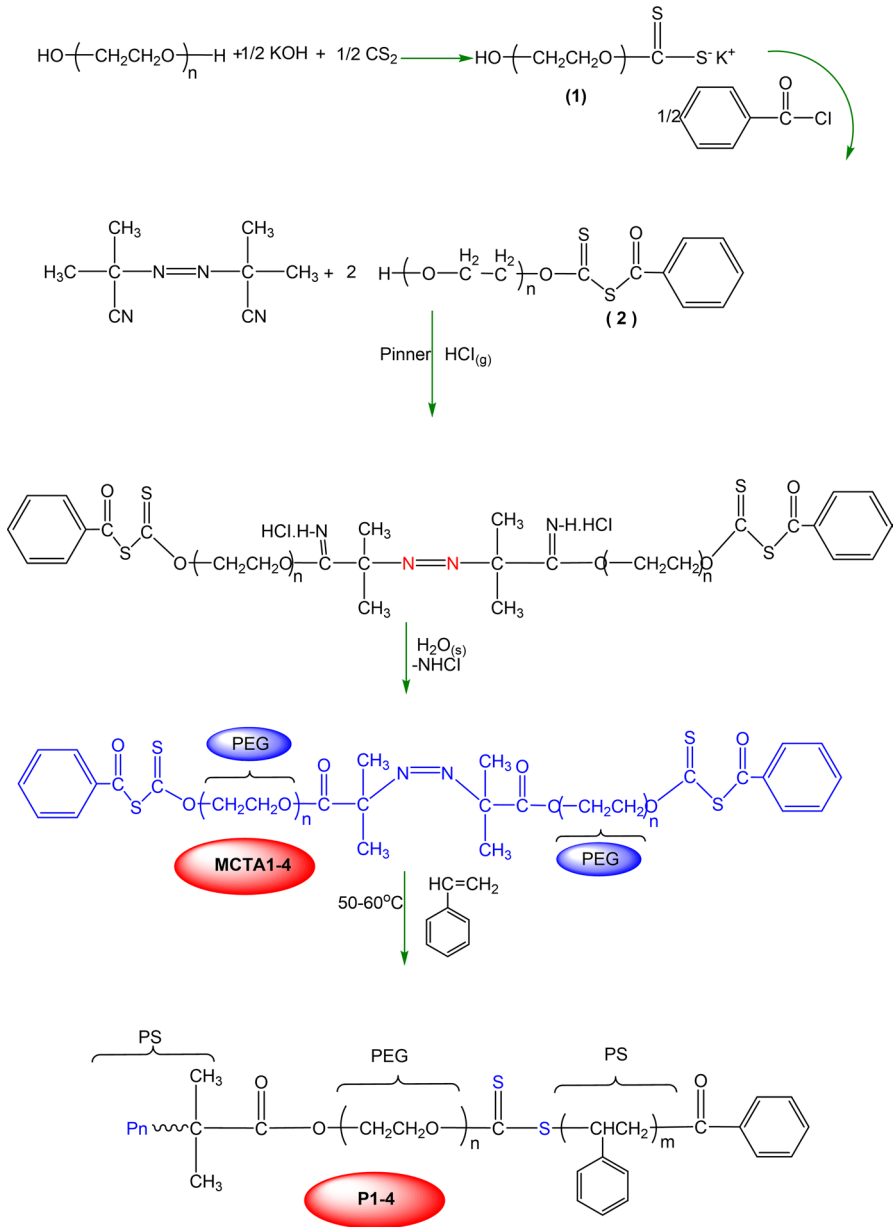
(2H, $-\text{OCH}_2$), 3.5–3.3 (4H, $-\text{CH}_2\text{CH}_2-$), MCTA3 için 7.9–7.6 (4H, ArH), 4.5 (2H, $-\text{OCH}_2$), 3.6–3.4 (4H, $-\text{CH}_2\text{CH}_2-$) ve MCTA4 için 8.0–7.7 (4H, ArH), 4.5 (2H, $-\text{OCH}_2$), 3.7–3.3 (4H, $-\text{CH}_2\text{CH}_2-$). ^{13}C NMR (CDCl_3 , δ , ppm): MCTA2 için 167 (1C, C=S), 162 (1C, C=O), 132 (1C, C- CH_3), 128–120 (6C, Ar), 71 (2C, O- CH_2), 60 (2C, $-\text{CH}_2\text{CH}_2-$), 23–21 ($-\text{CH}_3$) (Figure S4–S5). MCTA3 için 166 (1C, C=S), 163 (1C, C=O), 133 (1C, C- CH_3), 129–127 (6C, Ar), 70 (2C, O- CH_2), 60 (2C, $-\text{CH}_2\text{CH}_2-$) 21–18 ($-\text{CH}_3$) (Figure S7–S8). MCTA4 için 167 (1C, C=S), 163 (1C, C=O), 141 (1C, C- CH_3), 132–128 (6C, Ar), 72 (2C, O- CH_2), 60 (2C, $-\text{CH}_2\text{CH}_2-$), 23–21 ($-\text{CH}_3$) (Figure S10–S11).

Polymerization of styrene with MCTA1 (P1), MCTA2 (P2), MCTA3 (P3), and MCTA4 (P4)

The initial molar ratio of each component was $[\text{St}] / [\text{MCTA1}] = 88/1$, respectively. MCTA1 (1730 g/mol) yield (3) 1.732 g (0.001 mol), $[\text{St}] / [\text{MCTA 2}] = 440/5$. MCTA2 (MW=2560 g/mol) yield (3) 2.50 g, $[\text{St}] / [\text{MCTA3}] = 440/5$. MCTA3 (MW=3560 g / mol) yield (3) 3.56 g and $[\text{St}] / [\text{MCTA4}] = 249/1$. MCTA4 (MW=6560 g / mol) yield (3) 2.2829 g. Each component was separately dissolved in 10 mL of benzene, and 10 mL of styrene (0.087 mmol) was added. The resulting mixtures were shared separately with 2 mL of solution and 10 stir bars per tube. The mixtures in the tube were degassed with argon gas. Tubes were tightly capped with a rubber chamber and placed in a thermostated silicone oil bath at 60–65 °C. The reaction started at 5, 10, 15, 20, 25, 30, 40, 45, and 50 h. After polymerization, PS-*b*-PEG-*b*-PS triblock copolymers were precipitated in 50–60 mL of methanol per tube. From the resulting copolymers, it were dried under vacuum at room temperature for 3 days to obtain a white solid (Scheme 1). FT-IR (ν , cm^{-1}): 3069 ($-\text{CH}$, Ar) for P1, 1674 ($-\text{C}=\text{O}$) 1086 ($-\text{C}=\text{S}$), 3069 ($-\text{CH}$, Ar) for P2, 1674 ($-\text{C}=\text{O}$) 1086 ($-\text{C}=\text{S}$), 3069 ($-\text{CH}$, Ar) for P3, 1674 ($-\text{C}=\text{O}$) 1086 ($-\text{C}=\text{S}$) and 3069 ($-\text{CH}$, Ar) for P4, 1674 ($-\text{C}=\text{O}$) 1086 ($-\text{C}=\text{S}$). ^1H NMR (CDCl_3 , δ , ppm): 7.5–6.8 (4H, ArH) for P1, 4.4 (2H, $-\text{OCH}_2$), 3.8–3.6 (4H, $-\text{CH}_2\text{CH}_2-$), 1.8–1.1 ($\text{CH}_2-\text{C}-\text{CH}_2$) (Figure S3), 7.3–6.7 (4H, ArH) for P2, 4.4 (2H, $-\text{OCH}_2$), 3.7–3.4 (4H, $-\text{CH}_2\text{CH}_2-$), 1.8–1.4 ($\text{CH}_2-\text{C}-\text{CH}_2$) (Figure S6), 7.5–7.1 for P3 (4H, ArH), 4.2 (2H, $-\text{OCH}_2$), 3.8–3.6 (4H, $-\text{CH}_2\text{CH}_2-$) 1.8–1.5 ($\text{CH}_2-\text{C}-\text{CH}_2$) (Figure S9), and 8.1–7.8 for P4 (4H, ArH), 4.4 (2H, $-\text{OCH}_2$), 3.7–3.5 (4H, $-\text{CH}_2\text{CH}_2-$), 2.1–1.8 ($\text{CH}_2-\text{C}-\text{CH}_2$) (Fig. S12).

Results and discussion

It is important to note that the synthesis of xanthate compounds containing macro-RAFT agents from the organic synthetic process is limited. In the design of the macro-RAFT agent RS (C=S) OZ, the appropriate selection of both the R and the Z group plays an important role in the rapid addition of the active polymeric radical and a high rate of fragmentation, respectively [24, 46, 47]. In the architecture of the MCTAs, we synthesized polymer blocks of the PEG series



Scheme 1 Synthetic pathways of MCTA1-4 and RAFT polymerization of styrene via MAI-RAFT agent

with a molecular weight of 600, 1000, 1500, and 3000 g/mol. Also, as an advantage, the RAFT agent is capable of producing thermally radicals with azo-initiator properties. As the RAFT agent difunctional xanthate, it advances the controlled radical mechanism from both sides.

Macro-radicals are more affected by the R group than the Z group in chemical bonding to the C=S double bond on thiocarbonyl thio transfer agent. The binding activity of the Z group varies in the following order: Z = aryl > alkyl > S-alkyl > O-alkyl > N, N-dialkyl [48]. Following that description, the benzoyl group was chosen as the R group to reinitiate styrene polymerization. In our system, all copolymerization experiments were carried out in a homogeneous solution medium, but the free radical initiator was not used. The azo-initiator group presented in the structure of the agents provides the radical source. Then, ABA triblock type and well-defined statistical PS-PEG-PS block copolymers (P1-4) were synthesized under the control of MCTA1-4 using styrene monomer. Tables 1 and 2 summarize the experimental conditions and the characteristics of the three-block copolymers obtained in solution polymerization of styrene with MADIX. Theoretical molecular weights of block copolymers can be calculated according to the following equation [29]:

$$Mn_{(Theo)} = \frac{[M]}{[MCTA]} \times \text{Conversion} \times MW_{\text{styrene}} + MWM_{CTA}$$

where [M] is the molar concentration of styrene, [MCTA] is the molar concentration of MCTA, MW styrene is the molecular weight of monomer, and MWM_{CTA} is the molecular weight of MCTA. The theoretical molecular weights of the block copolymers and the molecular weights determined by the GPC calculated showed good compatibility. A comparison of GPC spectra for block copolymers is given in Fig. 1. It is also presented in detail in support information (Figure S13–S16).

Table 1 PS-PEG-PS (P 1–2) characteristics were obtained for graft copolymerization of styrene with macro-MCTA 1 and MCTA 2 at 60 °C

Entry	Time (hours)	Substance Amount	ln [M] ₀ /[M]	^c M _{theoric} (g/mol)	^d M _{GPC} (g/mol)	^d Đ M _w /M _n	^e Conversion%
^a P6P 1	5	0.3129	0.4219	6966	30,651	1.45	35
P6P 2	10	0.4652	0.7169	13,392	32,600	1.5	51
P6P 3	35	0.8253	2.3851	37,662	34,816	1.42	90
P6P 4	45	0.8936	4.0779	46,212	36,862	1.43	98
P6P 5	50	0.900	5.6065	48,272	37,371	1.43	99
^b P10P 1	10	0.3771	0.5359	10,047	31,403	1.4	42
P10P 2	25	0.7529	1.7618	33,212	33,076	1.41	83
P10P 3	35	0.8264	2.3983	39,362	34,407	1.42	91
P10P 4	45	0.9688	4.6151	42,962	34,507	1.42	99

^aEach polymerization was performed in benzene using MCTA 1 (PEG 600-RAFT agent)

^bEach polymerization was performed in benzene using MCTA 2 (PEG 1000-RAFT agent)

^cM_{n, theo} = ([styrene] / [MCTA] x Mw(styrene) x Conv.) + Mw (MCTA))/2

^dDetermined through GPC in THF eluent using polystyrene standards

^eCalculated by gravimetric results

Table 2 PS-PEG-PS (P 3–4) characteristics obtained for graft copolymerization of styrene with macro-MCTA 3 and MCTA 4 at 60 °C

Entry	Time (hours)	Substance Amount	$\ln [M]_0/[M]$	$^c M_{\text{theoric}}$ (g/mol)	$^d M_{\text{GPC}}$ (g/mol)	$^d \overline{D} M_w/M_n$	e Conversion %
^a P15P 1	5	0.3614	0.5068	10,482	23,354	1.28	39.76
P15P 2	10	0.5323	0.8808	18,832	29,046	1.37	58.56
P15P 3	20	0.7774	1.9325	36,187	31,136	1.38	85.52
P15P 4	35	0.8384	2.5553	40,262	35,664	1.47	92.23
P15P 5	50	0.8467	2.6803	42,522	42,041	1.37	93.15
^b P30P 1	5	0.5246	0.8606	21,518	31,299	1.42	57.71
P30P 2	10	0.6348	1.1984	24,667	32,538	1.42	69.83
P30P 3	15	0.7475	1.7278	27,887	35,091	1.40	82.23
P30P 4	25	0.8658	3.0465	31,267	37,161	1.41	95.24
P30P 5	40	0.8924	4.0029	32,027	39,064	1.4	98.17
P30P 6	45	0.9075	6.4068	32,458	40,209	1.4	99.83

^aEach polymerization was performed in benzene using MCTA 3 (PEG 1500-RAFT agent)

^bEach polymerization was performed in benzene using MCTA 4 (PEG 3000-RAFT agent)

^c $M_n, \text{theo} = ([\text{styrene}] / [\text{MCTA}] \times M_w(\text{styrene}) \times \text{Conv.}) + M_w(\text{MCTA}) / 2$

^dDetermined through GPC in THF eluent using polystyrene standards

^eDetermined by gravimetric results

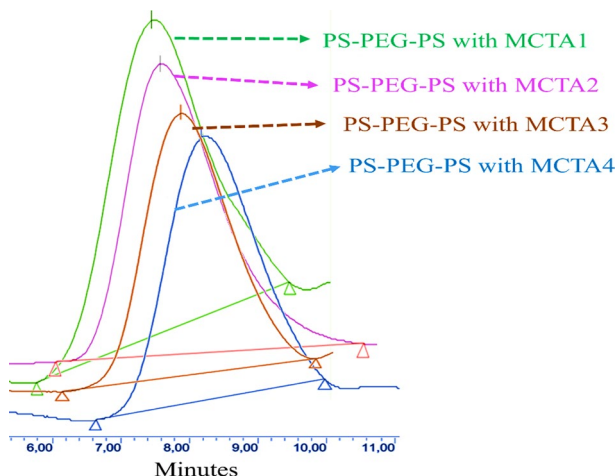


Fig. 1 GPC Analysis diagram of PS-PEG-PS block copolymer via MCTA 1–4

Macro-RAFT agents

After removing the PEG 600, KOH, CS₂, and benzoyl chloride were added to a monofunctional xanthate. The macro-RAFT agent (MCTA1-4) with azo initiator was obtained by a single side macro-RAFT agent. The success of controlled radical

RAFT polymerization is dependent on the synthesis of the chain transfer agent [49–52]. In this study, using the molecular weight of 600, 1000, 1500, and 3000 g/mol PEG series, we synthesized MAI-RAFT agents MCTA1-4.

Polymerization of styrene by synthesized MAI-RAFT agents

The most important function of RAFT polymerization is to perform molecular weight control [51–53]. Another function is to achieve close polydispersity ($\text{Đ} = 1$) [49–52]. In our study, the PDI values were ranging from 1.35 to 1.45 for all macro-RAFT polymerization. Copolymers (P1, P2, P3, and P4) with different molecular weights were synthesized in RAFT polymerization by controlling with MCTA1-4 agent. All the polymerization data were plotted using Origin 2018 programs.

The block copolymers were characterized by DSC techniques. The glass transition temperature (T_g) of the block copolymers was measured by differential scanning calorimetry (DSC), and the results are shown in Fig. 2. DSC studies showed that T_g values were around 86.9 °C, 85.8 °C, 84.1 °C, and 59.1 °C. The reason for the high decrease in T_g in the graph of P4 is the effect of the PEG block. The structural changes that occur

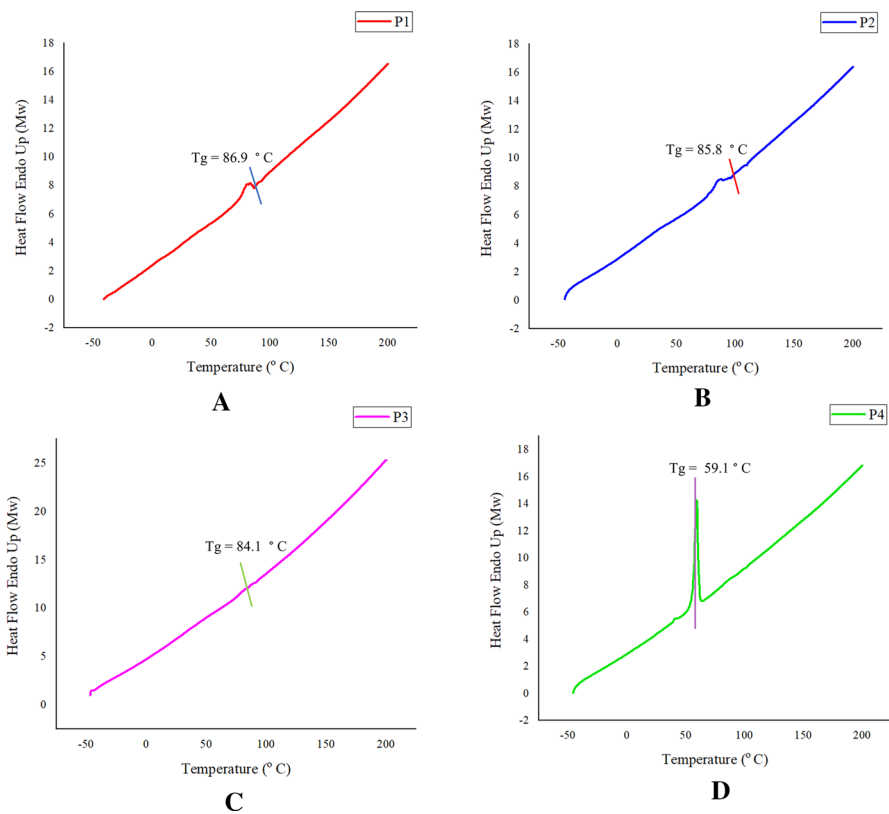


Fig. 2 The data of styrene polymerization with MCTA1-4 agent were compared values of DSC

Scheme 2 **a** Initiation and growth step of the controlled radical polymerization mechanism of styrene with MCTA1-4 agents. **b** The re-initiation and termination of the controlled radical polymerization mechanism of styrene with the MADIX agents

are highly dependent on the composition of the copolymer. Transitions between 50 and 90 °C can be attributed to relaxations and concomitant changes in the organization of the PEG segments. In Fig. 2, the typical DSC scan appeared as a different peak in a range (For P4) that disappeared upon heating.

Mechanism of MAI-RAFT polymerization of styrene

Initiation

The reaction I entails a two-step initiation mechanism, while the generation of initiating RAFT agent radicals $P_1\bullet$ via thermal effect. (Scheme 2a) Produced $P_1\bullet$ radicals initiate new polymeric chains $P_n\bullet$, but also it may terminate before escaping the solvent cage and form inactive products. Thus, radical initiation has an initiator efficiency of f ($0 < f < 1$) [54]. Value f usually decreases with the conversion of $[M]$ which becomes lower and viscosity becomes higher. The radical source of the reaction occurs in this step. RAFT agent radical $P_n\bullet$ was formed by monomers addition [55].

Reversible chain transfer

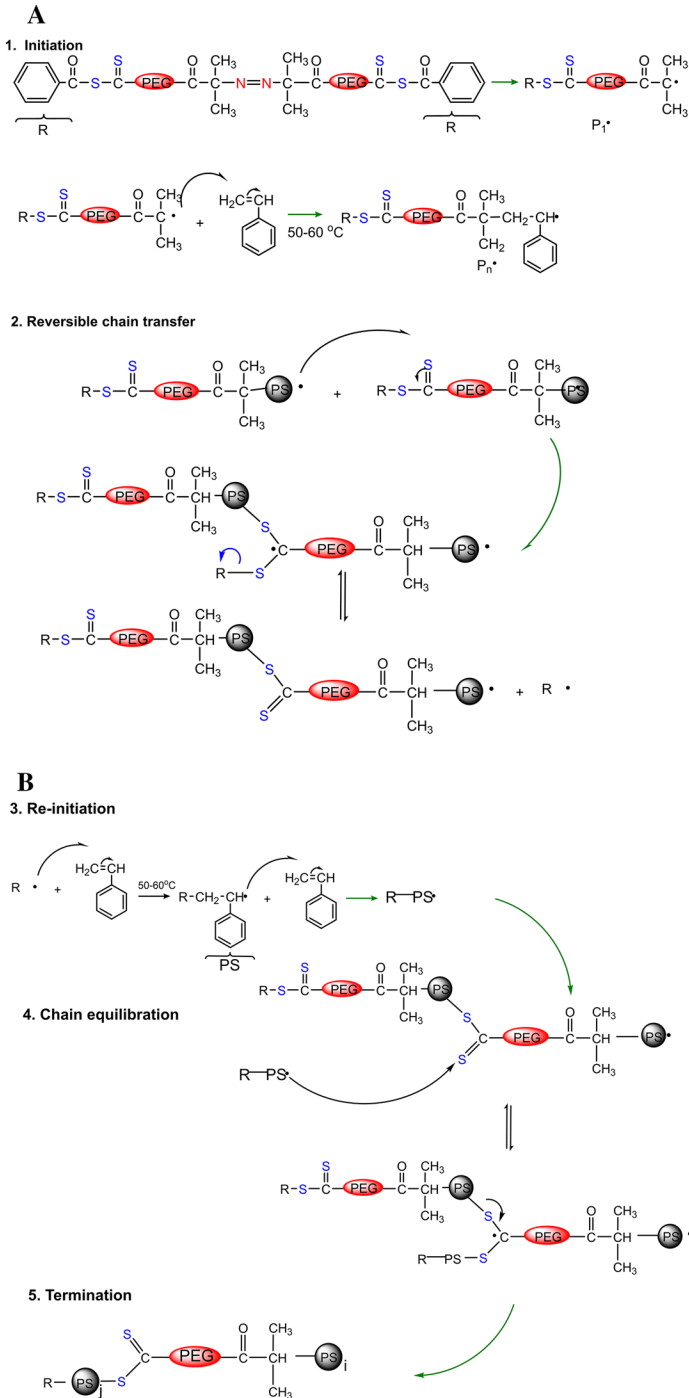
The growth step was similar to a conventional RAFT polymerization, but it was slightly different because obtained MADIX agent radical had two tasks. First, this agent was used together with the thiocarbonyl compound to control the polymerization. The second task was the addition of a large number of styrene to the active radical center ($P_n\bullet$). These reactions performed a degenerative chain transfer mechanism.

Re-initiation

Resulting in a reversible reaction, the obtained benzoyl radical ($-R\bullet$) group reacted with existent styrene in solution and formed different active polymer chain radicals. That is why the leaving group of the original MADIX agent (i.e., the R group) needs to be chosen in such a way that it is a better hemolytic leaving group than the polymer chain (P_n) [56, 57]. The net result of this sequence of the forward reactions was the generation of a new polymer (oligomer) chain ($R-PS\bullet$).

Main equilibrium: chain-to-chain transfer

A bond was formed between the growing active macro-MADIX radical group and the R-PS radical. All of this forward reaction sequence showed an addition-fragmentation cycle [55].



Termination

RAFT polymerization termination step is suppressed by a decrease in radical concentration [58]. The termination was achieved by stopping the reaction mixture manually. Thus, styrene monomer was removed by actively growing chains. In the termination step, the block copolymer of PS-PEG-PS was obtained. Reaction step V represents the conventional termination reaction. However, in the current Scheme 2b, it shows not only combination termination but also the termination of the growing PS block on the initiator. Both reactions are generally considered chain length dependent, but in an effective working MADIX reaction, both PS blocks are almost the same size ($i \approx j$).

Kinetic studies of controlled polymerization of styrene were performed in the presence of xanthate type MCTA 1–4 containing azo initiator in benzene at 60 °C. As shown in Figs. 3d and 4d, the styrene polymerization rate was faster in the presence of MCTA 4. According to these plots (Figs. 3, 4 and 5) in the polymerization PS-PEG-PS with MCTA 1–4, the rate constants were determined to be $k_1 = 1,81 \times 10^{-5}$, $k_2 = 3,35 \times 10^{-5}$, $k_3 = 2,3 \times 10^{-5}$, and $k_4 = 2,53 \times 10^{-5} \text{ s}^{-1}$, respectively. These values show that the chain length of the PEG block did not change the kinetics of the overall polymerization reaction rate. Furthermore, when monitored

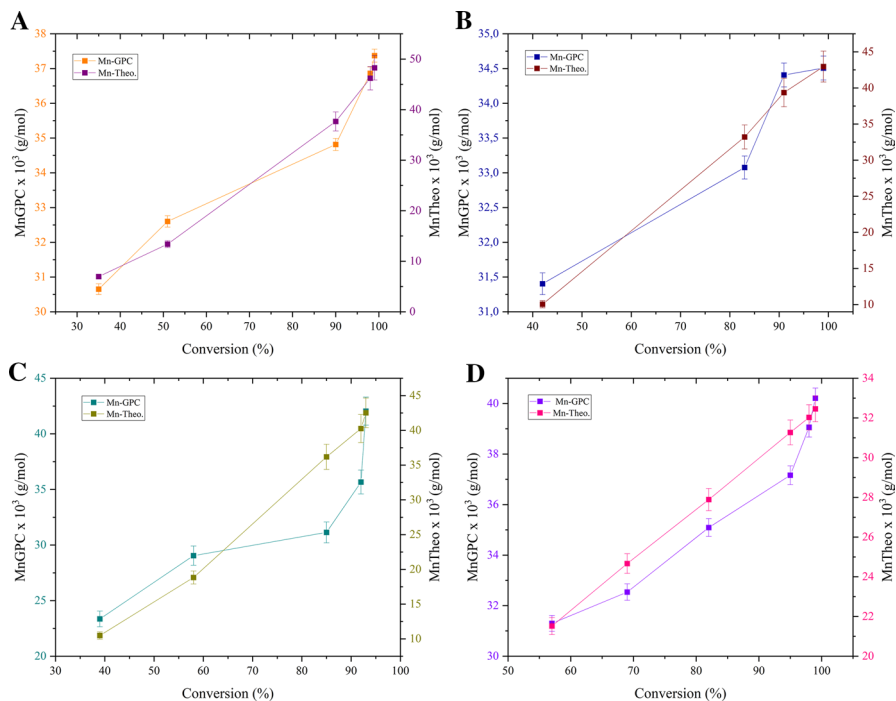


Fig. 3 Mn_{GPC} and Mn_{Theo} versus the conversion (%) with **a** MCTA 1 and **b** MCTA 2, **c**MCTA 3 and **d** MCTA 4

in Fig. 4a and b, the value of $\ln [M]_0/[M]$ versus the time graph showed that it was a first-order reaction rate.

Molecular weight and kinetic monitoring are the most important parameters among the performance and success of controlled/living radical polymerizations [59–63]. Concerning the control of molecular weight, the use of MCTA agents yielded favorable results (Figs. 3, 4, and 5). In all the polymerizations, depending on the reaction time, M_n (GPC) increased linearly with the monomer conversion following the live polymerization theory. The slope of the curve at 65 °C is linearly dependent on the conversion of styrene monomers. Thus, perfect control over the molecular weight was also observed. As seen in Fig. 5a and b, M_n (GPC) values are very close to M_n (theoretical) for all block copolymers. However, there are deviations in the first 5–10 h period of polymerization. This can be attributed to that the reaction reached high molecular weight in a controlled manner from the beginning. Besides, as the advantage of having the azo initiator in the MCTA structure, the initiator was not affected by the lattice effect and steric obstacles.

The ^1H NMR spectra of the macro-RAFT agents are shown the connected to the benzene ring $-\text{CH}_2$ protons at 1–2 ppm, the $-\text{CH}_3$ protons at 2.5 ppm (Fig. 6). The $-\text{CH}$ protons are shown between 7.5–8 ppm. RAFT agents, solvent, and CH_2 groups at 40 ppm in ^{13}C NMR spectra as seen in Fig. 7, $-\text{CH}$ groups at 75 ppm at CH_2

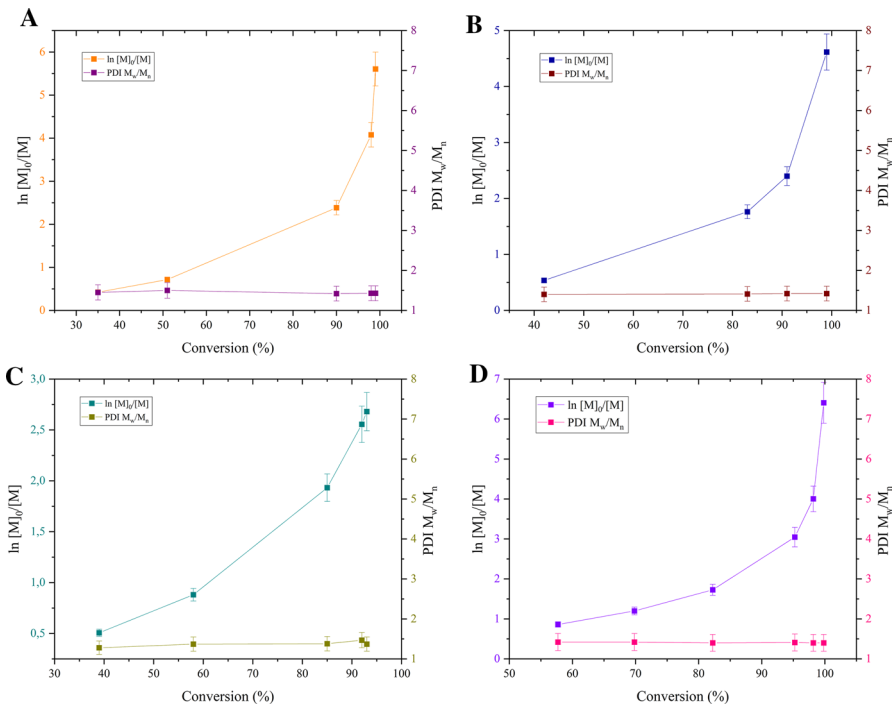


Fig. 4 $\ln [M]_0/[M]$ and PDI values versus the conversion (%) via **a** MCTA 1, **b** MCTA2, **c** MCTA 3 and **d** MCTA4 at $[M]_0/[MCTA]_0 = 166/2$ and thermal polymerization at 60–65 °C in benzene

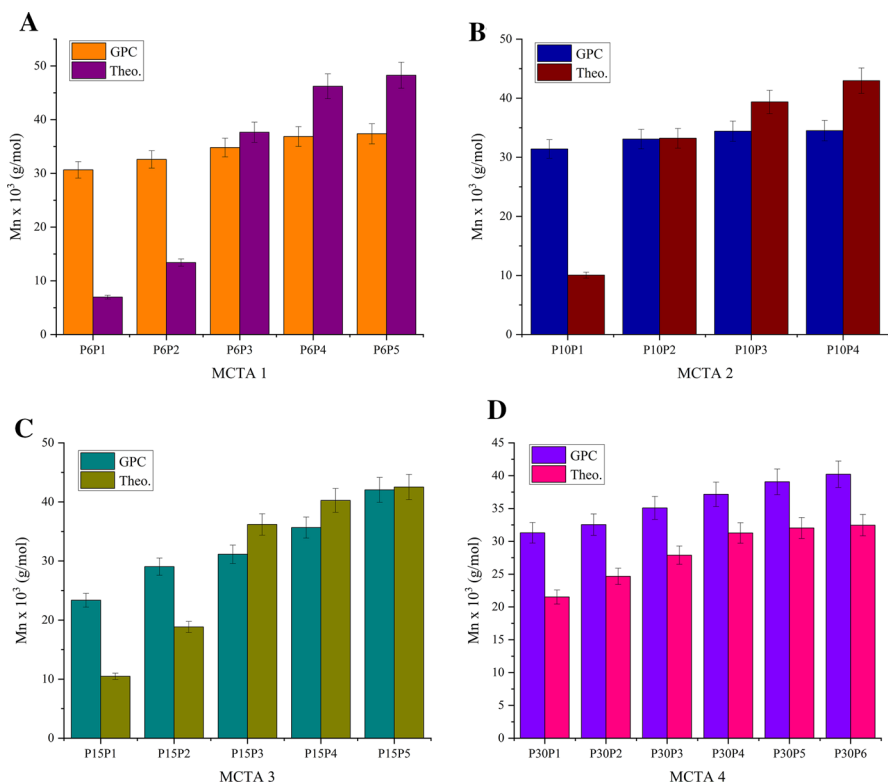


Fig. 5 Comparison graph between theoretical and GPC molecular weight with **a** MCTA 1, **b** MCTA 2, **c** MCTA 3 and **d** MCTA 4

groups at 130 ppm C=O groups at 135 ppm C=O at 170 ppm are observed. Peaks belonging to S groups are not apparent.

Conclusion

In this study, the synthesis of new macro-RAFT/MADIX agents with the azo initiator and different PEG blocks on both sides was accomplished with a new approach to prepare block copolymers. Controlled radical polymerization of styrene with the obtained MCTA 1–4 agents, and the molecular weights of PS-PEG-PS block

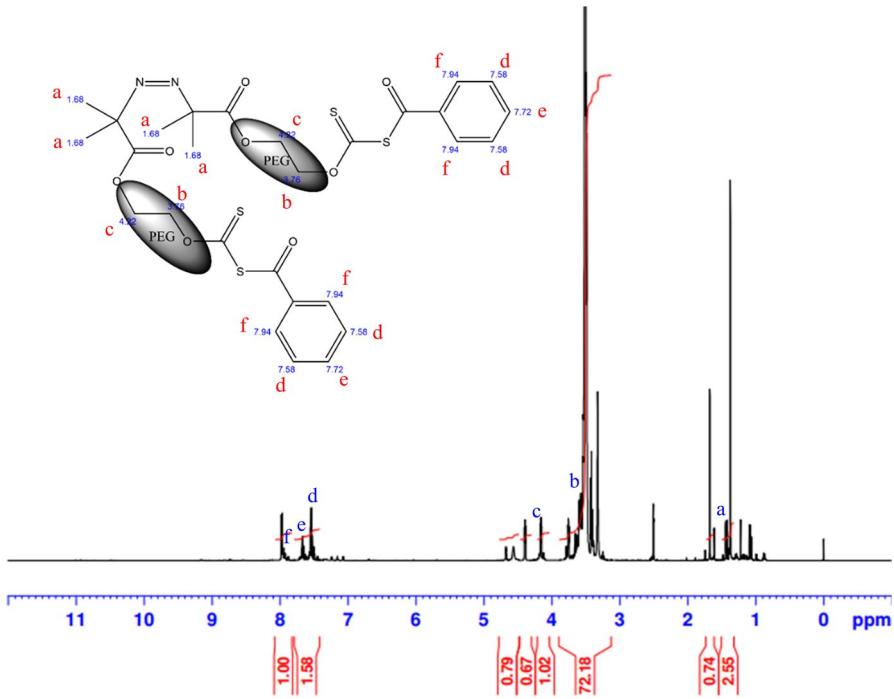


Fig. 6 ¹H-NMR spectrum of PS-PEG-PS with xanthate macro-RAFT agent (MCTA1)

copolymers ranging from 23,000 to 43000 g/mol, the polydispersity ($\mathcal{D} < 1.4$) was produced. In our system, it was created on the RAFT agent as the first source of radical. Then, the molecular control was achieved by polymeric chain growth and reversible chain transfers over the agent. The results of various analyses have been presented successfully in binding the RAFT polymerization at the targeted capacity and forming the block copolymer. Synthesized xanthate group with a difunctional and azo initiator makes the RAFT agent superior to conventional agents. By using controlled radical polymerization, we achieved a successful mechanism and good copolymers with good polydispersity.

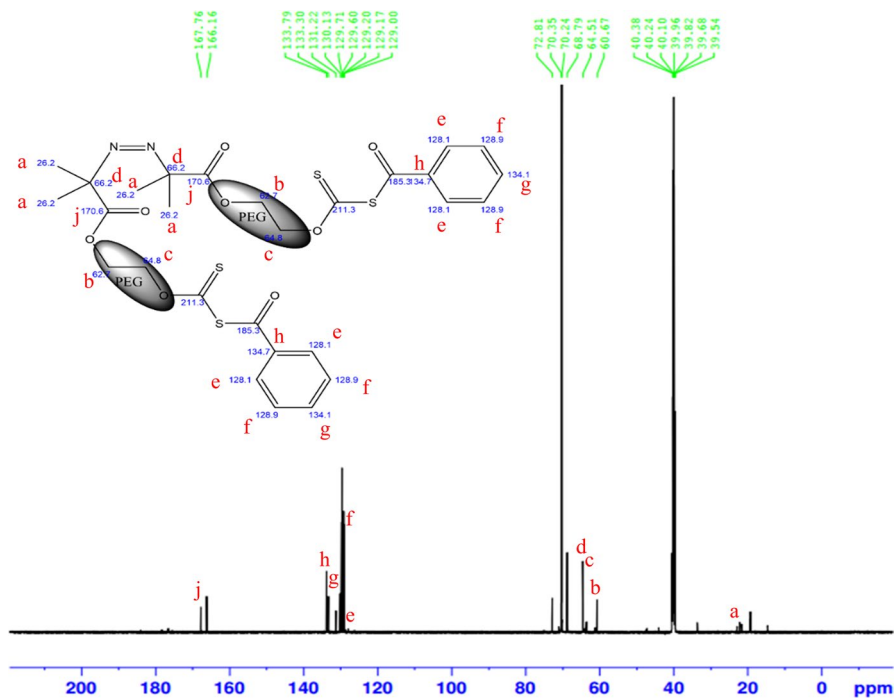


Fig. 7 ^{13}C -NMR spectrum of PS-PEG-PS with xanthate macro-RAFT agent (MCTA1)

Supplementary Information The online version contains supplementary material available at <https://doi.org/10.1007/s00289-021-03813-8>.

References

1. Yan M, Lin F-Y, Cochran EW (2017) Dynamics of hyperbranched polymers derived from acrylated epoxidized soybean oil. *Polymer* 125:117–125
2. Liu B, Kazlauciusas A, Guthrie JT, Perrier S (2005) One-Pot Hyperbranched Polymer Synthesis Mediated by Reversible Addition Fragmentation Chain Transfer (RAFT) Polymerization. *Macromolecules* 38(6):2131–2136
3. Dai B, Song M, Hourston DJ, He X, Liang H, Pan C (2004) Influence of block lengths and symmetries of block copolymers on phase behavior of polymer A/polymer B/block copolymer ternary blends. *Polymer* 45(3):1019–1026
4. Yang L, Luo Y, Liu X, Li B (2009) RAFT miniemulsion polymerization of methyl methacrylate. *Polymer* 50(18):4334–4342
5. West AG, Barner-Kowollik C, Perrier S (2010) Poly(ethylene glycol) as a ‘green solvent’ for the RAFT polymerization of methyl methacrylate. *Polymer* 51(17):3836–3842
6. Sugihara S, Iwata K, Miura S, Ma’Radzi AH, Maeda Y (2013) Synthesis of dual thermoresponsive ABA triblock copolymers by both living cationic vinyl polymerization and RAFT polymerization using a dicarboxylic RAFT agent. *Polymer* 54(3):1043–1052
7. Moad G, Rizzardo E (2020) A 20th anniversary perspective on the life of RAFT (RAFT coming of age). *Polym Int* 69:658–661

8. Nicolas J, Guillauneuf Y, Lefay C, Bertin D, Gignes D, Charleux B (2013) Nitroxide-mediated polymerization. *Prog Polym Sci* 38(1):63–235
9. Métafiot A, Pruvost S, Gérard J-F, Defoort B, Marić M (2020) Synthesis of isoprene-based triblock copolymers by nitroxide-mediated polymerization. *Eur Polym J* 134:109798
10. Neugebauer D (2015) Two decades of molecular brushes by ATRP. *Polymer* 72:413–421
11. Beija M, Marty J-D, Destarac M (2011) RAFT/MADIX polymers for the preparation of polymer/inorganic nanohybrids. *Prog Polym Sci* 36(7):845–886
12. Messina MS, Messina KMM, Bhattacharya A, Montgomery HR, Maynard HD (2020) Preparation of biomolecule-polymer conjugates by grafting-from using ATRP, RAFT, or ROMP. *Prog Polym Sci* 100:101186
13. Braunecker WA, Matyjaszewski K (2007) Controlled/living radical polymerization: Features, developments, and perspectives. *Prog Polym Sci* 32(1):93–146
14. Evci M, Tevlek A, Aydin HM, Caykara T (2020) Synthesis of temperature and light sensitive mixed polymer brushes via combination of surface-initiated PET-ATRP and interface-mediated RAFT polymerization for cell sheet application. *Appl Surf Sci* 511:145572
15. Faghihi F, Hazendonk P (2017) RAFT polymerization, characterization, and post-polymerization modification of a copolymer of vinylbenzyl chloride: Towards thiolate functionalized copolymers. *Polymer* 128:31–39
16. Gurnani P, Perrier S (2020) Controlled radical polymerization in dispersed systems for biological applications. *Prog Polym Sci* 102:101209
17. Ding L, Li Y, Cang H, Li J, Wang C, Song W (2020) Controlled synthesis of azobenzene-containing block copolymers both in the main- and side-chain from SET-LRP polymers via ADMET polymerization. *Polymer* 190:122229
18. Moad G, Rizzardo E, Thang SH (2008) Radical addition-fragmentation chemistry in polymer synthesis. *Polymer* 49(5):1079–1131
19. Chen F, Cheng Z, Zhu J, Zhang W, Zhu X (2008) Synthesis of poly(vinyl acetate) with fluorescence via a combination of RAFT/MADIX and “click” chemistry. *Eur Polym J* 44(6):1789–1795
20. Zhang S, Chen K, Liang L, Tan B (2013) Synthesis of oligomer vinyl acetate with different topologies by RAFT/MADIX method and their phase behaviour in supercritical carbon dioxide. *Polymer* 54(20):5303–5309
21. Yeole N, Hundiwale D (2011) Effect of hydrophilic macro-RAFT agent in surfactant-free emulsion polymerization. *Colloids Surf A Physicochem Eng Asp* 392(1):329–334
22. Dommanget C, D’Agosto F, Monteil V (2014) Polymerization of Ethylene through Reversible Addition-Fragmentation Chain Transfer (RAFT). *Chem Int Ed* 126(26):6801–6804
23. Barsbay M, Güven O (2018) Nanostructuring of polymers by controlling of ionizing radiation-induced free radical polymerization, copolymerization, grafting and crosslinking by RAFT mechanism. *Radiat Phys Chem* 169:107816
24. Barthet C, Wilson J, Cadix A, Destarac M, Chassenieux C, Harrisson S (2018) Influence of sodium dodecyl sulfate on the kinetics and control of RAFT/MADIX polymerization of acrylamide. *J POLYM SCI POLY CHEM* 56(7):760–765
25. Perrier S, Takolpuckdee P (2005) Macromolecular design via reversible addition-fragmentation chain transfer (RAFT)/xanthates (MADIX) polymerization. *J POLYM SCI POLY CHEM* 43(22):5347–5393
26. Hakobyan K, Gegenhuber T, McErlean CSP, Müllner M (2019) Visible-Light-Driven MADIX Polymerisation via a Reusable, Low-Cost, and Non-Toxic Bismuth Oxide Photocatalyst. *Angew Chem Int Ed* 58(6):1828–1832
27. Congdon TR, Notman R, Gibson MI (2017) Synthesis of star-branched poly(vinyl alcohol) and ice recrystallization inhibition activity. *Eur Polym J* 88:320–327
28. Bernard J, Favier A, Davis TP, Barner-Kowollik C, Stenzel MH (2006) Synthesis of poly(vinyl alcohol) combs via MADIX/RAFT polymerization. *Polymer* 47(4):1073–1080
29. Uyar Z, Turgut F, Arslan U, Durgun M, Degirmenci M (2019) Synthesis and characterization of well-defined end-chain functional macrophotoinitiators of polystyrene and polyacrylonitrile by RAFT/MADIX polymerization. *Eur Polym J* 119:102–113
30. Roy D, Sumerlin BS (2011) Block copolymerization of vinyl ester monomers via RAFT/MADIX under microwave irradiation. *Polymer* 52(14):3038–3045
31. Tastet D, Save M, Charrier F, Charrier B, Ledeuil J-B, Dupin J-C, Billon L (2011) Functional bio-hybrid materials synthesized via surface-initiated MADIX/RAFT polymerization from renewable natural wood fiber: Grafting of polymer as non leaching preservative. *Polymer* 52(3):606–616

32. Kartal B, Yildiko U, Ozturk S, Ata AC, Cakmak I (2014) Study of Solution Polymerization of Styrene in the Presence of Poly(ethylene glycol)-RAFT Agents Possessing Benzoyl Xanthate Derivatives. *J POLYM SCI POL CHEM* 51(12):990–998
33. Wang Y, Hu L, Yin Q, Du K, Zhang T, Yin Q (2020) Supporting data for the photo-induced deformation behavior for AZO-containing polymers connected by hydrogen bonding. *Data Br* 28:104849
34. Zhang CL, Zhang DF, Zhao HY, Lin ZY, Huang HH (2012) A facile protocol for N-Cbz protection of amines in PEG-600. *CCL* 23(7):789–792
35. Ganapathi M, Jayaseelan D, Guhanathan S (2015) Microwave assisted efficient synthesis of diphenyl substituted pyrazoles using PEG-600 as solvent – A green approach. *Ecotoxicol Environ Saf* 121:87–92
36. Balwe SG, Lim KT, Cho BG, Jeong YT (2017) A pot-economical and green synthesis of novel (benzo[d]imidazo[2,1-b]thiazol-3-yl)-2H-chromen-2-one in ethanol–PEG-600 under catalyst-free conditions. *Tetrahedron* 73(25):3564–3570
37. Czech Z, Butwin A, Herko E, Hefczyk B, Zawadiak J (2008) Novel azo-peresters radical initiators used for the synthesis of acrylic pressure-sensitive adhesives. *EXPRESS Polym Lett* 2:277–283
38. Tasdelen MA, Durmaz YY, Karagoz B, Bicak N, Yagci Y (2008) A new photoiniferter/RAFT agent for ambient temperature rapid and well-controlled radical polymerization. *J POLYM SCI POL CHEM* 46(10):3387–3395
39. Nagamune T, Nagai S, Ueda A (1996) Synthesis of (AB)_n-type block copolymers employing surface-active macro-azo initiators. *J Appl Polym Sci* 62(2):359–365
40. Lee EJ, Park HJ, Kim SM, Lee KY (2018) Effect of Azo and Peroxide Initiators on a Kinetic Study of Methyl Methacrylate Free Radical Polymerization by DSC. *Macromol Res* 26(4):322–331
41. Cvetkovska M, Lazarevic M, Koseva S, Baysal B, Hamurcu EE, Uyanik N (1997) Macro-azo-initiators having poly(ethylene glycol) units: Synthesis, characterization, and application to AB block copolymerization. *J Appl Polym Sci* 65(11):2173–2181
42. Nakamura K, Fujimoto K, Kawaguchi H (1999) Dispersion polymerization of methyl methacrylate using macro-azo-initiator. *Colloids Surf A Physicochem Eng Asp* 153(1):195–201
43. Simonova YA, Topchiy MA, Filatova MP, Yevlampieva NP, Slyusarenko MA, Bondarenko GN, Asachenko AF, Nechaev MS, Timofeeva LM (2020) Impact of the RAFT/MADIX agent on protonated diallylammonium monomer cyclopolymerization with efficient chain transfer to monomer. *Eur Polym J* 122:109363
44. Moad G, Rizzardo E, Thang SH (2012) Living Radical Polymerization by the RAFT Process – A Third Update. *Aust J Chem* 65(8):985–1076
45. Yang Y, Qiu S, Xie X, Wang X, Li RKY (2010) A facile, green, and tunable method to functionalize carbon nanotubes with water-soluble azo initiators by one-step free radical addition. *Appl Surf Sci* 256(10):3286–3292
46. Aerts A, Lewis RW, Zhou Y, Malic N, Moad G, Postma A (2018) Light-Induced RAFT Single Unit Monomer Insertion in Aqueous Solution—Toward Sequence-Controlled Polymers. *Macromolecules* 39(19):1800240
47. Levere ME, Chambon P, Rannard SP, McDonald TO (2017) MADIX polymerization of vinyl acetate using ethyl acetate as a green solvent; near-complete monomer conversion with molecular weight control. *J POLYM SCI POL CHEM* 55(15):2427–2431
48. Destarac M (2011) On the Critical Role of RAFT Agent Design in Reversible Addition-Fragmentation Chain Transfer (RAFT) Polymerization. *Polym Rev* 51(2):163–187
49. Marcilli RHM, Camilo APR, Petzhold CL, Felisberti MI (2018) Amphiphilic diblock copolymers based on sucrose methacrylate: RAFT polymerization and self-assembly. *J Mol Liq* 266:628–639
50. Kim T, Mays J, Chung I (2018) Porous poly(ϵ -caprolactone) microspheres via UV photodegradation of block copolymers prepared by RAFT polymerization. *Polymer* 158:198–203
51. Chen Q, Han F, Lin C, Wen X, Zhao P (2018) Synthesis of bioreducible core crosslinked star polymers with N, N'-bis(acryloyl)cystamine crosslinker via aqueous ethanol dispersion RAFT polymerization. *Polymer* 146:378–385
52. Ishigaki Y, Mori H (2018) Synthesis of poly(chloroprene)-based block copolymers by RAFT-mediated emulsion polymerization. *Polymer* 140:198–207
53. Levit M, Zashikhina N, Dobrodumov A, Kashina A, Tarasenko I, Panarin E, Fiorucci S, Korzhikova-Vlakh E, Tennikova T (2018) Synthesis and characterization of well-defined

- poly(2-deoxy-2-methacrylamido-d-glucose) and its biopotential block copolymers via RAFT and ROP polymerization. *Eur Polym J* 105:26–37
54. Barner-Kowollik C, Buback M, Charleux B, Coote ML, Drache M, Fukuda T, Goto A, Klumperman B, Lowe AB, Mcleary JB, Moad G, Monteiro MJ, Sanderson RD, Tonge MP, Vana P (2006) Mechanism and kinetics of dithiobenzoate-mediated RAFT polymerization. I. The current situation. *J Polym Sci Pol Chem* 44(20):5809–5831
 55. Moad G (2019) A Critical Survey of Dithiocarbamate Reversible Addition-Fragmentation Chain Transfer (RAFT) Agents in Radical Polymerization. *J POLYM SCI POL CHEM* 57(3):216–227
 56. Sandeau A, Mazières S, Destarac M (2012) Well-defined macromolecular architectures through consecutive condensation and reversible-deactivation radical polymerizations. *Polymer* 53(25):5601–5618
 57. Mun H, Hwang K, Kim W (2019) Synthesis of emulsion styrene butadiene rubber by reversible addition–fragmentation chain transfer polymerization and its properties. *Journal of Appl Polym Sci* 136(7):47069
 58. Zhou D, Zhu X, Zhu J, Hu L, Cheng Z (2007) 2-oxo-tetrahydrofuran-3-yl 9H-carbazole-9-carbodithioate mediated reversible addition-fragmentation chain transfer (RAFT) polymerization. *J Appl Polym Sci* 104(5):2913–2918
 59. Couture G, Améduri B (2012) Kinetics of RAFT homopolymerisation of vinylbenzyl chloride in the presence of xanthate or trithiocarbonate. *Eur Polym J* 48(7):1348–1356
 60. Guan C-M, Luo Z-H, Qiu J-J, Tang P-P (2010) Novel fluorosilicone triblock copolymers prepared by two-step RAFT polymerization: Synthesis, characterization, and surface properties. *Eur Polym J* 46(7):1582–1593
 61. Lowe AB, McCormick CL (2007) Reversible addition–fragmentation chain transfer (RAFT) radical polymerization and the synthesis of water-soluble (co)polymers under homogeneous conditions in organic and aqueous media. *Prog Polym Sci* 32(3):283–351
 62. Vora A, Singh K, Webster DC (2009) A new approach to 3-miktoarm star polymers using a combination of reversible addition–fragmentation chain transfer (RAFT) and ring opening polymerization (ROP) via “Click” chemistry. *Polymer* 50(13):2768–2774
 63. York AW, Kirkland SE, McCormick CL (2008) Advances in the synthesis of amphiphilic block copolymers via RAFT polymerization: stimuli-responsive drug and gene delivery. *Adv Drug Deliv Rev* 60(9):1018–1036

Publisher's Note Springer Nature remains neutral with regard to jurisdictional claims in published maps and institutional affiliations.